


[Submit your article ↗](#) Menu Search in this journal

The 6th International Conference on Advanced Materials Science and Technology 2018(6th ICAMST), Semarang, Indonesia, 9-10 October 2018

Edited by Abdul Latif binAhmad, Khairurrijal K, Kuwat Triyana, Hadi Nur, Hutomo Suryo Wasisto, Markus Diantoro

Volume 13, Part 1,
Pages 1-316 (2019)

 [Download full issue](#)

[← Previous vol/issue](#)[Next vol/issue >](#)

Receive an update when the latest issues in this journal are published

 [Sign in to set up alerts](#)

Research article Abstract only

[FEEDBACK !\[\]\(4f6bf54ae7e4144a72d78316053e412d_img.jpg\)](#)

[Submit your article](#) ↗Research article Abstract only

Applying Pulse Height Analysis (PHA) Technique on an Optical Particle Counter (OPC) using Commercial ADC Module

Dian Ahmad Hapidin, Widya Sinta Mustika, Casmika Saputra, Dian Syah Maulana, ... Muhammad Miftahul Munir

Pages 252-257

[Article preview](#) ✓Research article Abstract only

Study on Morphology and Crystal Structure of Pd Doped $\text{Nd}_{1.2}\text{FeO}_3$

Eko Hadi Sujiono, Vicran Zharvan, Muhammad Yusriadi Dahlan, Andi Chaerunnisa Mugni Said, ... Samnur

Pages 258-263

[Article preview](#) ✓Research article Abstract only

$\text{Nd}(\text{Fe})_{0.3}\text{Ba}_{1.7}\text{Cu}_3\text{O}_{7.8}$ Oxide Material Crystal Structure and Morphological Analysis

Eko Hadi Sujiono, Awalia Husnul Khatimah, Aisyah Nur Hasanah, Nurul Fitriyah Mahendi, ... Andi Irhamsyah

Pages 264-269

[Article preview](#) ✓Research article Abstract only

Study of Craters Morphology and Projectile Deformation from Ballistic Tests using Firearms on the Body Plate of Vehicle

Happy Riyono, Agus Suprihanto, Sulisty, Rusnaldy

Pages 270-275

[Submit your article](#) ↗Research article Abstract only

Simulation Load Parameter on Bipolar Artificial Hip Joint Using Finite Element Method (FEM)

Reza Azizul Nasa Al Hakim, Ahmad Edwan, Jamari Jamari, Rifky Ismail, ... Sakuri Dahlan
Pages 305-310

[Article preview](#) ✓Research article Abstract only

Performance Stability and Optical Properties of *Musa Acuminata* bracts-based Dye-Sensitized Solar Cell

Sutikno Madnasri, Syaikhul Hadi, Rieza Dwi Ayu Wulandari, Ian Yulianti, ... Dhidik Prastiyanto
Pages 311-316

[Article preview](#) ✓[← Previous vol/issue](#)[Next vol/issue >](#)

ISSN: 2214-7853

Copyright © 2023 Elsevier Ltd. All rights reserved

ICAMST 2018

Study on Morphology and Crystal Structure of Pd Doped $\text{Nd}_{1.2}\text{FeO}_3$

Eko Hadi Sujiono^{a,*}, Vicran Zharvan^a, Muhammad Yusriadi Dahlan^a,
Andi Chaerunnisa Mugni Said^a, Jasdar Agus^a, Samnur^a

^aLaboratory of Material Physics. Department of Physics, Universitas Negeri Makassar, Makassar 90223, Indonesia

Abstract

Study on morphology and crystal structure of $\text{Nd}_{1.2}\text{Pd}_x\text{Fe}_{1-x}\text{O}_3$ doped Pd (1,2,3,4 and 5 wt%) synthesized by solid state reaction method have been investigated. X-ray diffraction (XRD) and scanning electron microscope (SEM) were used to identify phase and morphology of sample. Further analysis using *X'Pert High Score Plus* software show that samples have two phases: $\text{Nd}_{1.2}\text{Pd}_x\text{Fe}_{1-x}\text{O}_3$ as major phase and Nd_2O_3 as a minor phase. $\text{Nd}_{1.2}\text{Pd}_x\text{Fe}_{1-x}\text{O}_3$ crystalline size obtained by Scherrer equation has a value ranging from 43 to 50 nm and also has spherical shapes with the small existence of Pd confirmed by EDS results.

© 2019 Elsevier Ltd. All rights reserved.

Peer-review under responsibility of the scientific committee of The 6th International Conference on Advanced Materials Science and Technology 2018, 6th ICAMST.

Keywords: palladium; NdFeO_3 ; morphology; crystal structure; crystalline size

1. Introduction

The ReFeO_3 (Re: rare-earth elements) as known as the rare-earth orthoferrites has an orthorhombic structure derived from a perovskite structure [1]. These rare-earth orthoferrites have attracted much interest due to their properties such as magnetic and magneto-optic [2]. Further, NdFeO_3 material also can be used as raw material of gas sensors[3], fuel cells[4] and catalyst material gas sensors [5-6]. The preparation of NdFeO_3 material can be achieved by several methods including a high-temperature ceramic method, hydrothermal synthesis [7], sol-gel method [8] and many more.

* Corresponding author. Tel.: +62-81-14105272
E-mail address: e.h.sujiono@unm.ac.id

Among those several methods, the solid-state reaction method was selected to synthesized the NdFeO_3 material because this method is cheap and easy to achieve. Furthermore, the product of the reaction has high purity and good crystallinity [9]. Perovskite materials such as NdFeO_3 give a good opportunity to improve its properties by varying their chemical composition [10-11]. The ReFeO_3 can be doped with other metals to increase its properties such as Ni-doped GdFeO_3 , Co-doped LaFeO_3 , Mn-doped LuFeO_3 but less information about using noble elements such as palladium as a doping material in NdFeO_3 .

In this paper, the Palladium (Pd) doped NdFeO_3 samples were prepared by using a solid-state reaction method. The Pd that used was varied from 1, 2, 3, 4 and 5 wt%. All samples of $\text{Nd}_{1.2}\text{Pd}_x\text{Fe}_{1-x}\text{O}_3$ then characterized to obtain their crystal structure properties and morphology. Further, the Refinement results also presented using the Rietveld method.

2. Experimental method

In this paper, the Pd doped $\text{Nd}_{1.2}\text{FeO}_3$ sample was synthesized by the following process. The first process, raw materials of Nd_2O_3 (Strem Chemicals, 99.99%), Pd_2O_3 (Sigma-Aldrich, 99.99%) and Fe_2O_3 (Sigma-Aldrich, 99.99%) were mixed and ground using mortar for 3 hours. That mixed material then calcined using an electric furnace at 700°C for 6 hours. The calcined sample was milled for 5 hours following by sintering at 950°C for 6 hours.

The sintered material was ground for 3 hours and recalined at 950°C for 6 hours. The material then ground for 5 hours and sintered at 1050°C for 9 hours. Those procedures were then implemented for different Pd content from 1 to 5 wt%.

The phase of $\text{Nd}_{1.2}\text{Pd}_x\text{Fe}_{1-x}\text{O}_3$ samples was characterized using XRD (Rigaku Mini Flex II $\text{CuK}\alpha$, $\lambda = 0.154 \text{ nm}$) and SEM-EDAX (FEI Inspect S50) to obtain the phase and morphology, respectively.

3. Results and discussions

3.1. Analysis of x-ray diffraction patterns

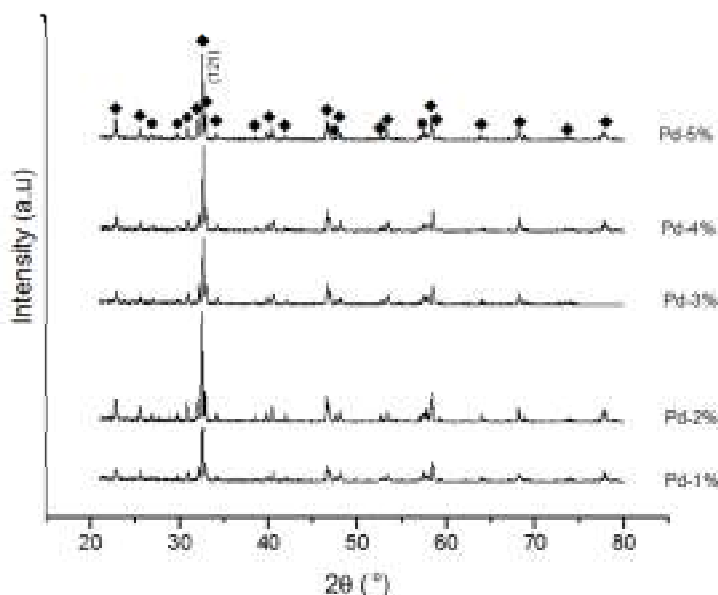


Fig. 1. X-ray diffraction pattern of Pd doped $\text{Nd}_{1.2}\text{FeO}_3$ (◆ = $\text{Nd}_{1.2}\text{Pd}_x\text{Fe}_{1-x}\text{O}_3$, ● = Nd_2O_3)

Fig. 1. shows the result of X-ray diffraction characterization for $\text{Nd}_{1.2}\text{Pd}_x\text{Fe}_{1-x}\text{O}_3$ samples. Analysis using X'Pert High Score Plus software shows that all of $\text{Nd}_{1.2}\text{Pd}_x\text{Fe}_{1-x}\text{O}_3$ ($x = 1, 2, 3, 4$ and $5 \text{ wt}\%$) compounds crystallize as

perovskite phase with orthorhombic structure with two major phases: $\text{Nd}_{1.2}\text{Pd}_x\text{Fe}_{1-x}\text{O}_3$ and Nd_2O_3 with the highest peak lead to $\text{Nd}_{1.2}\text{Pd}_x\text{Fe}_{1-x}\text{O}_3$ phase at plane (121) in orthorhombic structure for each sample which is similar to previous results [9,12-13]. Fig.1. also shows the presence of Nd_2O_3 phase. The presence of Nd_2O_3 phase due to the low temperature during the calcination process [9] and Nd_2O_3 which did not react perfectly with Fe_2O_3 to form NdFeO_3 [19]. There is no peak of impurity observed which indicates that the samples consist of pure phases [14].

Fig. 2. shows information about the relative intensity of $\text{Nd}_{1.2}\text{Pd}_x\text{Fe}_{1-x}\text{O}_3$ phase and Nd_2O_3 . It can be seen that the presence of palladium in the lattice of $\text{Nd}_{1.2}\text{FeO}_3$ has a significant effect on the relative intensity of the sample. The highest intensity lies to sample with palladium content at 3 wt% which explain the best crystallinity.

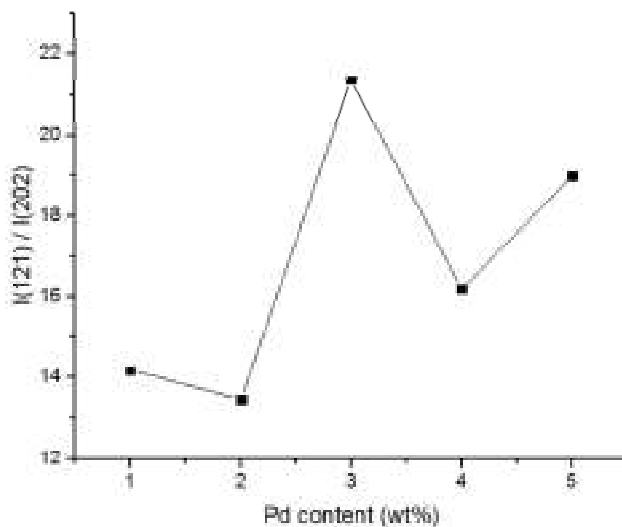


Fig. 2. Relative intensity of $\text{Nd}_{1.2}\text{Pd}_x\text{Fe}_{1-x}\text{O}_3$ phase at $2\theta = 32.56^\circ$ and Nd_2O_3 phase at $2\theta = 64.08^\circ$ as a variation of palladium content

Further analysis of Pd doped $\text{Nd}_{1.2}\text{FeO}_3$ is presented in Table 1. It is observed that the peak position of (121) Bragg's plane lower as Pd content increases. It indicates that the expansion of the lattice parameters occurs [15] due to the diffusion of ion Pd^{3+} into NdFeO_3 mother compound [16] substituting the Fe^{3+} ion. The crystalline size of the samples can be obtained using the Debye–Scherrer equation (1) [17]:

$$D = \frac{0.89\lambda}{\beta \cos(\theta)} \quad (1)$$

where λ is the wavelength of X-ray (0.15406 nm), β is FWHM value at (121), and θ is diffraction angle.

Table 1. X-ray analysis results of Pd doped $\text{Nd}_{1.2}\text{FeO}_3$ at plane (121)

Pd (%)	2θ (degree)	FWHM* (degree)	Crystalline size (nm)
1	32.6107	0.18948±0.00394	43.21
2	32.4937	0.16436±0.00394	43.80
3	32.5915	0.18473±0.00394	44.32
4	32.5843	0.16180±0.00394	50.60
5	32.4821	0.16376±0.00394	49.99

As shown in Table 1. the crystal size increase from 43.21 to 50.60 nm as the dopant increase from 1 to 4 wt%. A higher dopant does not make the lattice expand, but a little reduce. The nonlinear lattice expansion phenomena may be originated not only the ion substitution but more the limit of solid solubility.

Further analyses of the XRD histograms using Rietveld refinement method also interesting to be reported. The results of refinement are presented in Table 2. It is found that increasing of palladium content in $\text{Nd}_{1.2}\text{FeO}_3$ makes its

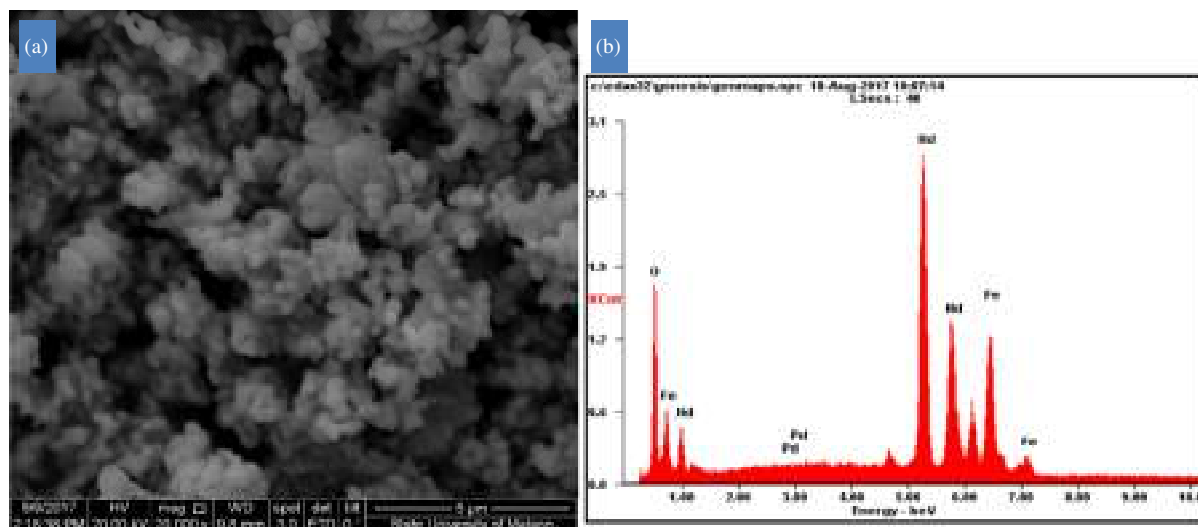
lattice parameter expand due to different ionic radii of Pd^{3+} which larger than Fe^{3+} ion. It also makes FWHM value decrease when the concentration of Pd increase to 5% and the crystalline size increase as the doping increase. The range of crystalline size of these samples is about 40 to 50 nm which has a similar value from another work [18]. Table 2. also gives the value of Goodness of Fit (GoF) for resulting refinement which in range of 0 to 1 indicating the fit patterns of between experimental data and model was good and acceptable [19-20].

Table 2. Lattice parameters of Pd doped $\text{Nd}_{1.2}\text{FeO}_3$ by Rietveld refinement

Pd Content (%)	a (Å)	b (Å)	c (Å)	Rp (%)	Rwp (%)	GoF (%)
1	5.581114 ± 0.001018	7.760299 ± 0.001435	5.449368 ± 0.000938	30.40	21.54	0.5
2	5.581471 ± 0.000908	7.764312 ± 0.001218	5.452063 ± 0.000816	30.24	19.67	1
3	5.582604 ± 0.001013	7.760463 ± 0.001473	5.450199 ± 0.000946	30.61	20.05	0.1
4	5.583977 ± 0.000774	7.761196 ± 0.001063	5.449952 ± 0.000697	31.05	21.35	0.7
5	5.584483 ± 0.000606	7.763024 ± 0.000827	5.453594 ± 0.000549	33.06	19.40	0.7

3.2. Analysis of morphology

Influence of palladium on the morphology of $\text{Nd}_{1.2}\text{FeO}_3$ was investigated by using SEM can be seen in Fig. 3. It is found that all of the samples show inhomogeneous morphology. This is indicated that increasing Pd^{3+} content on $\text{Nd}_{1.2}\text{FeO}_3$ does not significantly change the shape of grains, but change grain size larger. From the SEM images, we also observed that there are agglomerations occur. The sample with 1 wt% of palladium content exhibits more agglomerations than the sample with 5 wt%. It happens due to the small size of particles leading to the high surface area. This high surface area provides high surface energy, to minimize it the agglomeration is formed [21-22].



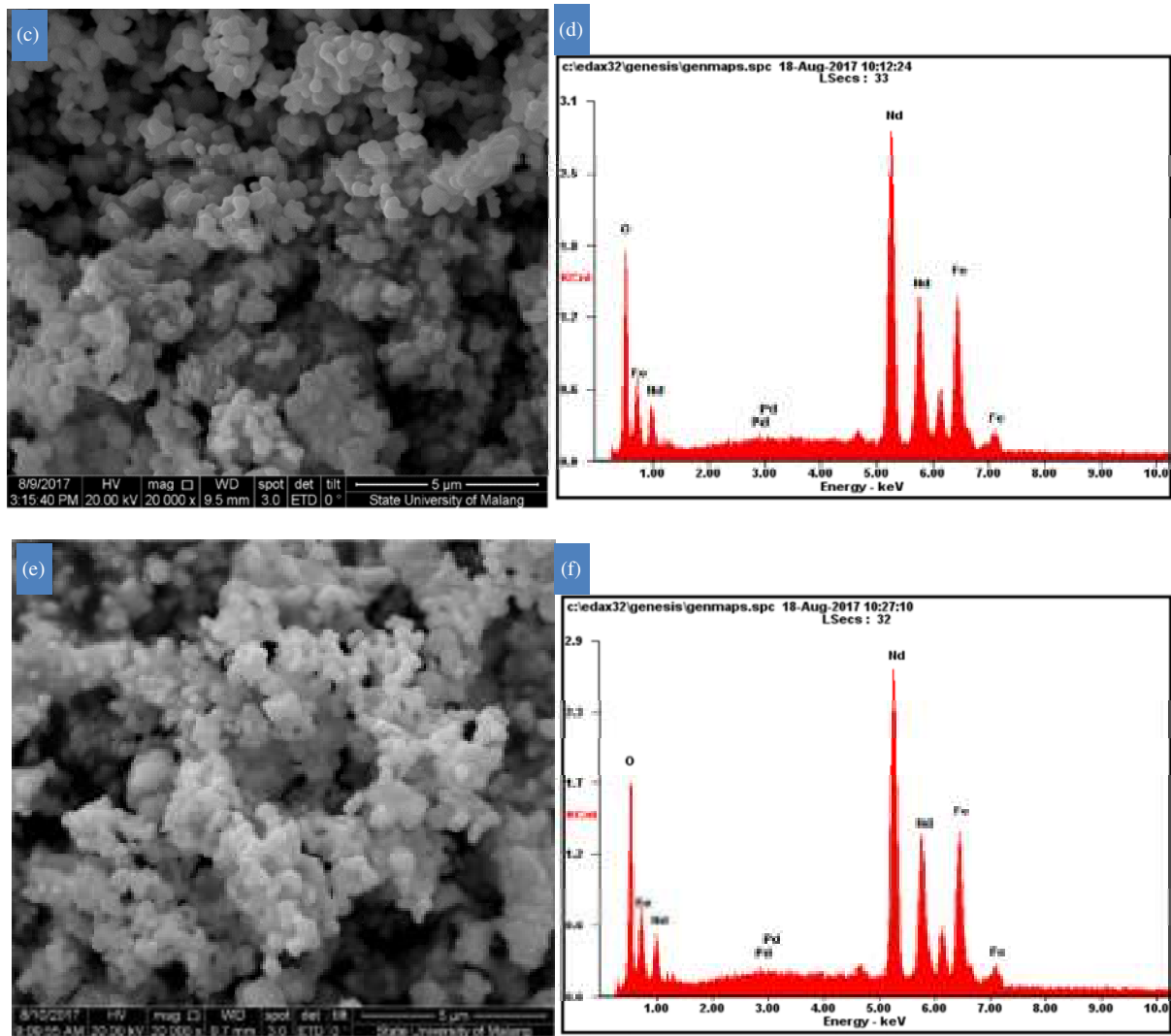


Fig. 3. Morphology of sample Pd doped Nd_{1.2}FeO₃ and its EDS spectrum at Pd doped: 1% (a – b); 3% (c – d); and 5% (e – f).

Further information of EDS results from all samples is listed in Table 3. It is interesting to see that the increase of Pd ion give rise to increase iron but decrease Nd ions. According to the ionic radii, the radius of Pd is closer to Fe ions rather than Nd ion. Table 3. explains that Pd substitution does not as simple as expected. A few amounts of Pd also could interstitially or substitute Nd ion. This result showed the presence of iron and neodymium as the dominant element. We also found the existent of palladium with a much lower fraction.

Table 3. The elemental composition of Nd_{1.2}FeO₃ from EDS measurement.

Pd content (%)	Elements (wt%)			
	O	Pd	Nd	Fe
1	12.36	00.23	69.72	17.69
2	12.02	00.30	70.23	17.44
3	12.66	00.53	68.04	18.77
4	13.47	00.65	66.49	19.40
5	12.92	00.80	67.19	19.09

Since the crystalline phase is mostly dominated by the $\text{Nd}_{1.2}\text{Pd}_x\text{Fe}_{1-x}\text{O}_3$ compare to Nd_2O_3 , as discussed previously. The elemental data also indicate that the Pd has been incorporated into the $\text{Nd}_{1.2}\text{FeO}_3$ into to two forms. The composite of $\text{Nd}_{1.2}\text{FeO}_3/\text{Nd}_2\text{O}_3$ and chemically substitute into $\text{Nd}_{1.2}\text{Pd}_x\text{Fe}_{1-x}\text{O}_3$. Therefore the main crystalline phase of the samples is $\text{Nd}_{1.2}\text{Pd}_x\text{Fe}_{1-x}\text{O}_3$ as confirmed using XRD, SEM and EDS results, respectively.

4. Conclusion

The Pd doped $\text{Nd}_{1.2}\text{FeO}_3$ samples were successfully synthesized by using a solid-state reaction method. The XRD analysis confirms that all samples exhibit an orthorhombic structure with two phases Nd_2O_3 and $\text{Nd}_{1.2}\text{Pd}_x\text{Fe}_{1-x}\text{O}_3$. The presence of Pd gradually shifted the 2θ into a lower 2θ degree. It causes because the Pd^{3+} ion successfully substitutes into $\text{Nd}_{1.2}\text{FeO}_3$ lattice replacing the Fe^{3+} ion due to the small difference of ionic radii to Pd^{3+} . According to the calculation, the average of the crystalline size of all samples ranging from 40.0-50.0 nm. Although Pd gives rise to effect on the crystal structure, it does not give significant effect to morphology. A further study is necessary to find the relation of pure phase Pd doped NdFeO_3 and its crystal structure.

Acknowledgments

This research was funded by Directorate research and Community Services, Directorate General of Research and Development, Ministry of Research, Technology and Higher Education, Republic of Indonesia, under research scheme of *Hibah Kompetensi* of 2017/2018.

References

- [1] W. Anhua, C. Guofeng, S. Hui, X. Jiayue, C. Yaoqing, G. Zengwei, Asia-Pac. J. Che. Eng. 4 (2009) 518-521.
- [2] Y. Mostafa, S. Z. Samanch, K. M. Mozghan, Curr Chem Lett. 6 (2017) 23-30.
- [3] N. Xinshu, D. Weimin, D. Weiping, J. Kai, J. Rare Earth. 6 (2003) 630.
- [4] S. Tongyun, S. Liming, J. Rare Earth. 30 (2012) 1138.
- [5] S. Taneja, Y. Nakamura, V. Garg, N. Hosoito, Nucl. Instrum. Method B.76 (1993) 127.
- [6] G. Song, J. Jiang, B. Kang, J. Zhang, Z. Cheng Solid State. Commun. 211 (2015) 47.
- [7] W. You, Y. Xuecheng, C. Jun, D. Jinxia, Y. Ranbo, X. Xianran, Cryst Eng Comm. 16 (2014) 858.
- [8] W. Zhan-Lei, Z. Ru, Z. Ma, F. Shao-Ming, H. Zhou-Xiang, H. Ji-Fan, W. Kai-Ying, Int J Min Met Mater. 2 (2010) 141.
- [9] V. Zharvan, Y. N. I. Kamaruddin, S. Samnur, E.H. Sujiono, IOP Conf Series: Materials Science and Engineering.202 (2017) 012072.
- [10] C.S. Vandana, J. Guravamma and B. H. Rudramadevi, IOP Conf Seeries: Materials Science and Engineering, 149 (2016).
- [11] E.H. Sujiono, A.C. Mugni-Said, M.Y. Dahlan, R.A. Imran, S. Samnur, Journal of Nano- and Electronic Physics. 10 (2018) 02034.
- [12] X. Lou, X. Jia, J. Xu, Journal of Rare Earths. 23 (2005) 328.
- [13] W. Yabin, C. Shixun, S. Mingjie, Y. Shujan, K. Baojuan, Z. Jincang, W. Anhua, X. Jun, J Cryst Growth. 318 (2011) 927-931.
- [14] T.S. Vijayakumar, S. Karthikeyan, S. Vasanth, A. Ganesh, G. Bupesh, R. Ramesh, M. Manimegalai, P. Subramanian, J. Nanosci. 2013.
- [15] K. Sultan, M. Ikram, K. Asokan, Vacuum. 99 (2014) 251-258.
- [16] M.B. Suwarnkar, R.S. Dhabbe, A.N. Kadam, K.M. Garadkar, Ceram Int. 40 (2014) 5489-5496.
- [17] T.G. Ho, T.D. Ha, Q.N. Pham, H.T. Giang, T.A.T. Do, T.T. Do, N.T. Nguyen. Sensors and Actuators B. 158 (2011) 246-251.
- [18] Z.L. Wu, R. Zhang, M. Zhao, S.M. Fang, Z.X. Han, J.F. Hu, K.Y. Wang, Int J Min Met Mater. 19 (2012) 141.
- [19] E.H. Sujiono, A.C.M. Said, M.Y. Dahlan, R.A. Imran, S.Samnur, IOP Conf. Series: Materials Science and Engineering.367 (2018) 012037.
- [20] B.H. Toby, Powder Diffr. 21 (2006) 1.
- [21] J. Jiang, G. Oberdosrster, P. Biswwas, J Nanopart Res. 11 (2009) 77-89.
- [22] A. Balakrishnan, P. Pizette, C.L. Martin, S.V. Joshi, B.P. Saha, Acta Materialia. 58 (2010) 802-812.